International Journal of Engineering Research & Technology (IJERT)
ISSN: 2278-0181
Vol. 4 Issue 10, October-2015

Flow Field Around Four Circular Cylinders – A Flow Visualization Study

B. H. Lakshmana Gowda, B. K. Srinivas,
J. Naveenkumar, T. R. Santhosh and D. Shamkumar
BTL Institute of Technology,
Department of Mechanical Engineering,
Bommasandra, Bengaluru – 560 099, India

Abstract **- The flow field around four circular cylinders in a square array is presented in this study. The spacing between the cylinders is varied systematically and at each spacing, the approach flow angle is varied. The flow patterns are visualized and the streamline patterns obtained. The results indicate that the gap flows have a predominant effect on the flow field and the resulting strong biased flows and vortex shedding may lead to different kinds of pressure fields and hence wind loads. The wake pattern and its extent are strongly dependent on the spacing between the cylinders and the orientation of the square array to the flow.**

Keywords: Square array, Circular cylinders, Interference effects, Spacing, Angle of attack.

INTRODUCTION

When flow takes place around a circular cylinder, over a range of Reynolds numbers, vortices are shed alternatively into the wake. Due to this, under certain conditions, the cylinder can be subjected to flow induced vibrations. An interfering cylinder either in front or behind can influence the amplitude of vibration considerably – the amplitude can increase or be suppressed depending on the relative position and size of the interfering cylinder. Zdravkovich, 1985, has studied the flow induced oscillations of two interfering circular cylinders. Gowda and Prabhu, 1987, Gowda and Deshkulkarni, 1987 and Gowda and Sreedharan, 1994, have investigated such interference effects with circular cylinders in various relative positions. Gowda et al., have studied the interference effects on the flow induced vibrations when three circular cylinders occur in a triangular array. Combinations of three and four circular section bodies are common in building aerodynamics. In the present study flow visualization results are obtained for a combination of four square cylinders (Fig.1) in a square array. The gap (g) between the circular cylinders is varied systematically and for each gap, results are obtained at different angle of attack (α).

EXPERIMENTAL ARRANGEMENT

Experiments have been conducted using the Flow Visualization Facility at the Fluid Mechanics Laboratory, Department of Mechanical Engineering, BTL Institute of Technology, Bengaluru. It consists of a FRP (Fibre Reinforced Plastic) tank 2.5 m in length, 1.5 m in width and 150 mm deep (Fig. 2). A set of aluminum discs separated by small distances are located at one end of the tank which are connected through a system of shaft and bevel gears to a induction motor with cooling arrangement. When the discs are rotated, they act as paddles and the flow created is guided into the test section (350 mm wide) through two guides (Fig.2). The test section width is 350 mm and by controlling the speed of the motor, the required speed in the test section could be obtained. For the present study, the circular cylinders with diameter (d) equal to 25 mm (Fig.1) made out of mild steel and painted black are used. The gap g is varied to get g/d values of 0, 0.2, 0.4, 0.6, 0.8 and 1. At each value of g/d, the cylinders fixed in the slots provided on a base plate are carefully turned in clockwise direction to achieve $\alpha = 0^0, 15^0, 30^0$ and 45^0. Considerable care was taken to achieve these positions with the help of accurately drawn lines on the top of the cylinder. All the results are obtained at a free stream velocity of 0.18 m/s which corresponds to a Reynolds number of 4500 referred to the diameter d. Fine aluminum powder is used as tracer medium and a single lens reflex (SLR) digital camera was located at a suitable height above the cylinders to photograph the flow field. Two 500 watt halogen lamps were used to get proper lighting.

RESULTS

At g/d=0 and α=0 (Fig 3a) the combination of cylinders is acting as a compound body. There is a regular vortex shedding behind the compound body. At α=15, (Fig 3b) this trend continues with the vortex shedding intensifying indicated by sinusoidal nature beyond the wake. At α=30 (Fig 3c) the intensity of vortex shedding appears to reduce. At α=45 (Fig 3d) there is a streamlining effect on the combination of cylinders and vortex width is minimum.

When the gap is g/d=0.2 (Fig 4a to d) the influence of the gap flow effect appears. At α=0 (Fig.4a), the flow is symmetrical with strong gap flows occurring between cylinders B-C and C-D, Coanda effect is seen around cylinders B-D (in the enclosed space between the cylinders) and due to the resulting bias effect of the gap flow the wake behind B-C are shortened and shifted to one side. The flow around front cylinder A indicates very little drag or lift forces on it. However, there is strong vortex shedding behind cylinder C indicating considerable periodic forces on the cylinders.

When α=15 (Fig 4b), there is further intensification of gap flow and slight shortening of wake behind B-D, compared to α=0. At α=30 i.e., angle of attack increases to 30 (Fig 4c), the bias in the gap flow reduces considerably (the gap flow is nearly straight) and the group of cylinders appears to act as one unit or compound body. This tendency continues at α=45 and vortex shedding appears to be controlled by the compound body rather than the gap flow.

At g/d=0.4 (Fig 5a and b) trends very similar to what is seen for g/d=0.2 at the corresponding angles are seen. However, at α=30 and 45 (Fig 5c and d) for this value (g/d=0.4) gap flow intensifies and pierces the wake to a larger extent. At α=45, there is nearly stagnant flow between cylinders A-D and B-C.

With further increase in g/d values to 0.6 (Fig.6 a to d), the trend seen at g/d=0.4 at α=0 and 15 (Fig 5a and b) intensifies. The wakes behind cylinders B and D become comparatively longer due to the dragging action of gap flow and stronger vortex shedding is seen behind cylinder C. At α=30, the gap flow impinging on cylinder C divides and moves down the gap flow between B-C. The incident flow on cylinder D moves around the cylinder (Coanda effect) and combines with the oncoming gap flow between cylinders A-B. At α=45 (Fig 6d), there is considerable cross flow between cylinders A-D and B-C. The bias in the gap flow almost disappears; there is streamlining effect, vortex activity in the wake reduces to a minimum.

For g/d=0.8 and above (Fig 7 and 8) vortex rolling is seen behind individual cylinders and periodic forces can be expected on all the cylinders. At α=15 (Fig 7b) cylinder C is subjected to strong oncoming gap flow and high stagnation pressure can be expected at front of C. At α=45 for both g/d=0.8 and 1 (Fig 7d and 8d respectively) there is a streamlining effect and the bias in the gap flow is minimum. The sheer layers on the gap side C&D are dragged along resulting in a narrower and longer wake behind cylinders C&D. The gap flow at these angles (α=45) extends into the wake region to a considerable distance. There is a channel like flow between the cylinders and beyond.

DISCUSSION

1) Considering the cases with gap g/d=0, it is seen that at α=15 (Fig.3b) there is strong vortex shedding on cylinder C which can result in considerable periodic forces. At α=45 (Fig.3d) there is a streamlining effect on the combination of cylinders and the extent of the wake appears to be minimum. The corresponding forces acting on this combination can be expected to be minimum.

2) At g/d=0.2, the gap flow effect is seen between the cylinders compared to g/d=0. At α=0 (Fig.4a), Coanda effect is seen behind cylinders B and D. Due to this effect wakes behind B and D are shortened. For α=45, the vortex shedding is controlled by the compound body.

3) As g/d increases further to 0.4, it is seen that the gap flow becomes stronger and particularly at α=30 (Fig.5c), the gap flow appears to pierce the wake to larger distance. At α=45 (Fig.5d) there is nearly stagnant fluid between A and D, and B and C.

4) A g/d=0.6, the gap flow becomes stronger and the wakes behind all the cylinders are affected in general. At α=45 (Fig.6d), there is considerable cross flow between cylinders A and D, B and C.The streamlining effect reduces the wake to a minimum.

5) For both g/d=0.8 and 1 (Figs.7 and 8), vortex rolling behind individual cylinders occur which can result in strong periodic forces on cylinders. At α=45 (Fig.7d and 8d), the gap flow extends far into the wake region and there is a channel like flow between the cylinders.

It is pointed out that it is difficult to measure the vortex shedding frequency for the different configurations, for which other methods have to be used.

CONCLUSIONS

The critical conditions, i.e., the probable configuration where either maximum periodic force can occur on the cylinders individually or in combination seems to depend both on g/d value and angle of attack. However, it is seen that for any gap g, at α=45, the wake tends to be minimum. This orientation may be considered safer compared to other situations.

REFERENCES

Gowda, B.H.L. and Prabhu, D.R., 1987. Interference effects on the flow-induced vibrations of a circular cylinder, Journal of Sound and Vibration 112, (3), 487-502.

Gowda, B.H.L. and Deshkulkarni,K.P.,1988. Interference effects on the flow-induced vibrations of a circular cylinder in side-by-side and staggered arrangement, Journal of Sound and Vibration 122, (3), 465-478.

Gowda, B.H.L. and Sreedharan,V., 1994. Flow induced oscillation of a circular cylinder due to interference effects, Journal of Sound and Vibration 176, 497-514.

Gowda, B.H.L., Prasad, B.V.S.S.S. and Anand,R.B.,2000.Vibratory response of a circular cylinder in triangular arrangement, Proceedings, 4th International Colloquium on Bluff Body Aerodynamics and Applications (4 BBAA), Bochum, Germany, 201-204.

Zdravkovich, M.M., Flow-induced oscillations of two interfering circular cylinders, 1985. Journal of Sound and Vibration 112, 511-521.

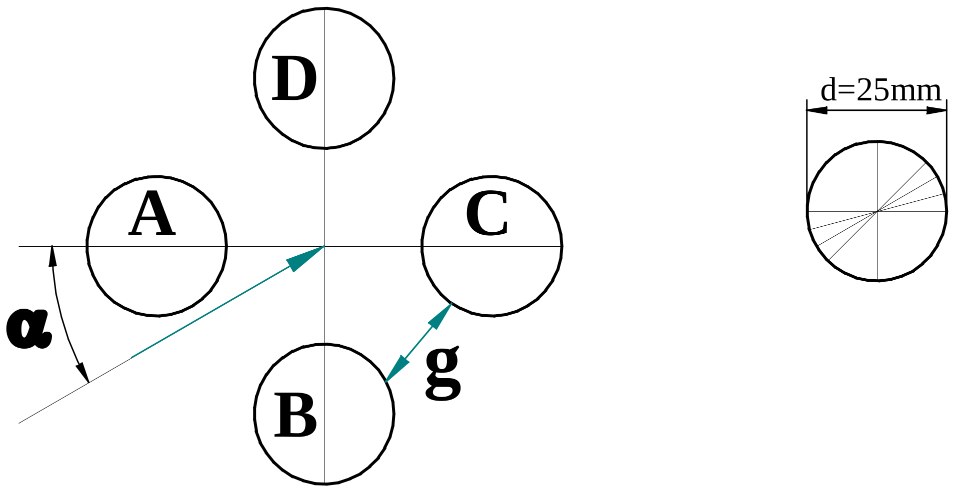

Fig.1 Configurations considered

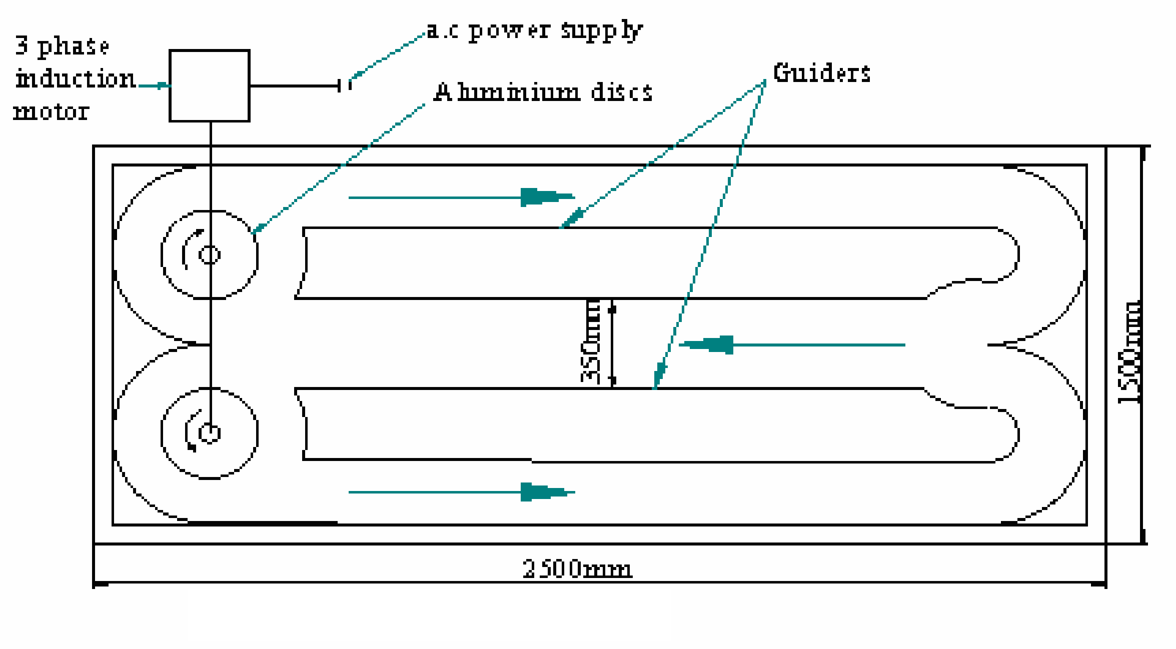

Fig.2. The experimental setup

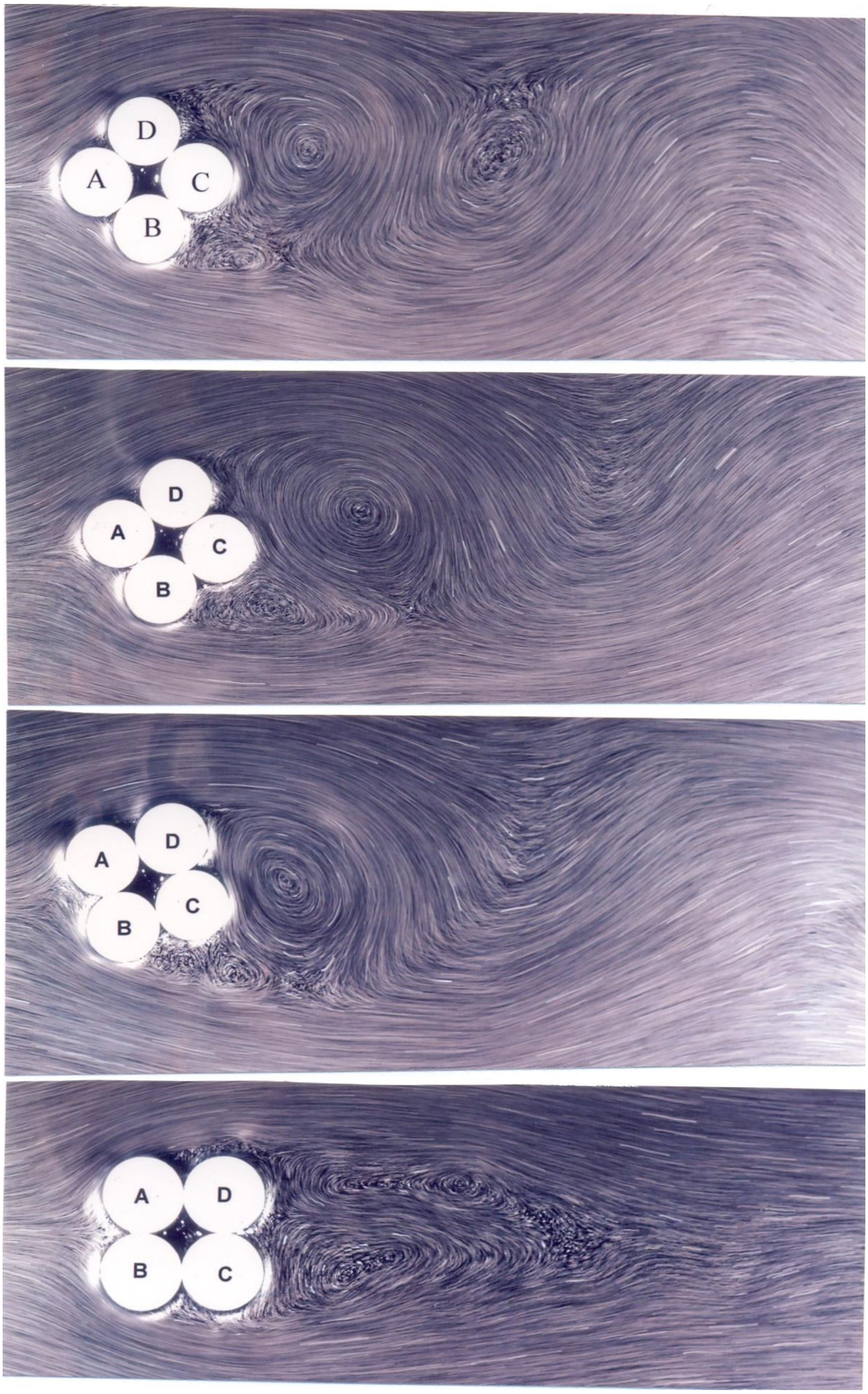

(a) $\alpha = 0^0$

(b) $\alpha = 15^0$

(c) $\alpha = 30^0$

(d) $\alpha = 45^0$

Fig.3 Flow pattern for various angle of attack α, g/d = 0

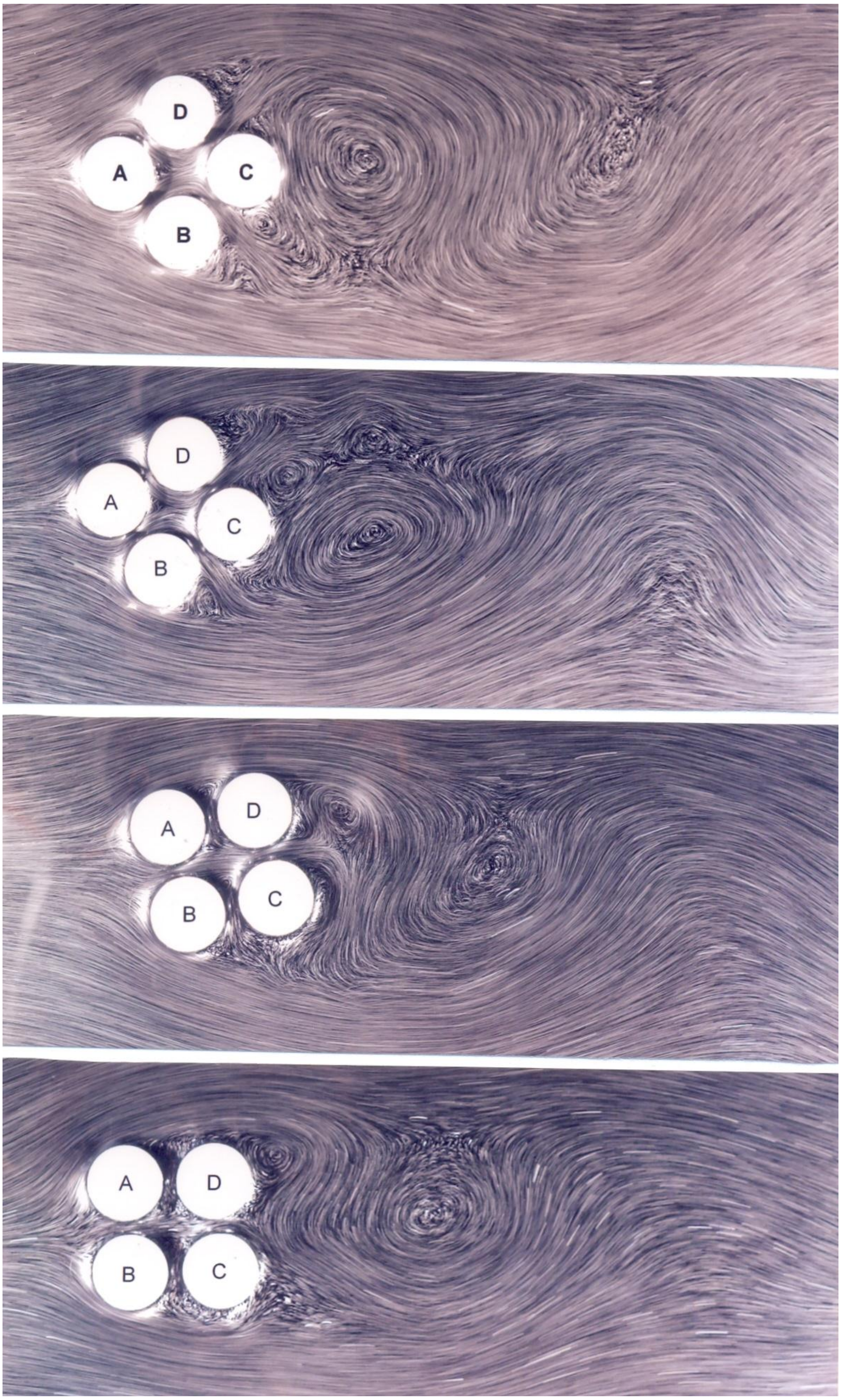

(a) $\alpha = 0^0$

(b) $\alpha = 15^0$

(c) $\alpha = 30^0$

(d) $\alpha = 45^0$

Fig.4 Flow pattern for various angle of attack α, g/d = 0.2

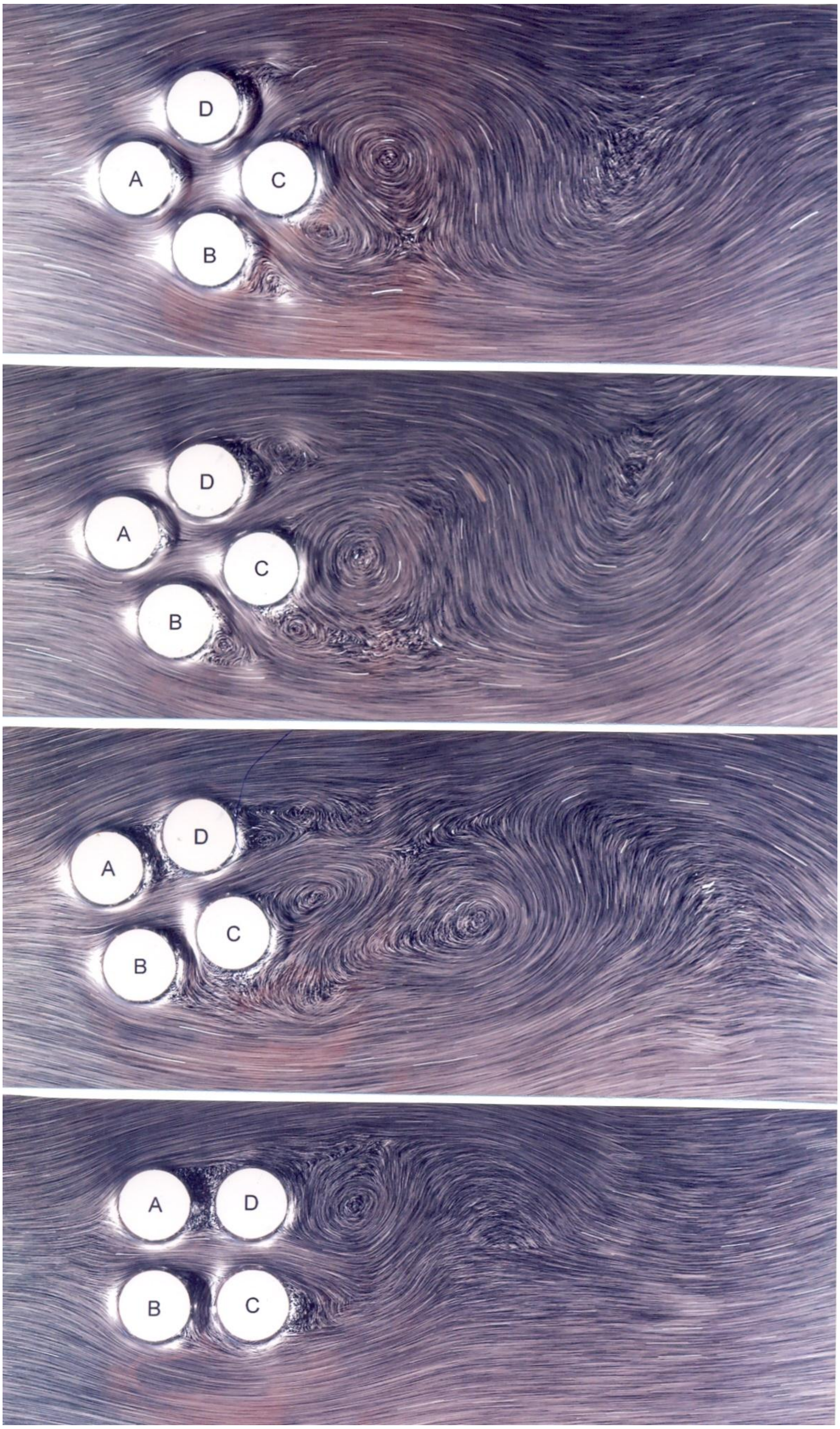

(a) $\alpha = 0^0$

(b) $\alpha = 15^0$

(c) $\alpha = 30^0$

(d) $\alpha = 45^0$

Fig.5 Flow pattern for various angle of attack α, g/d = 0.4

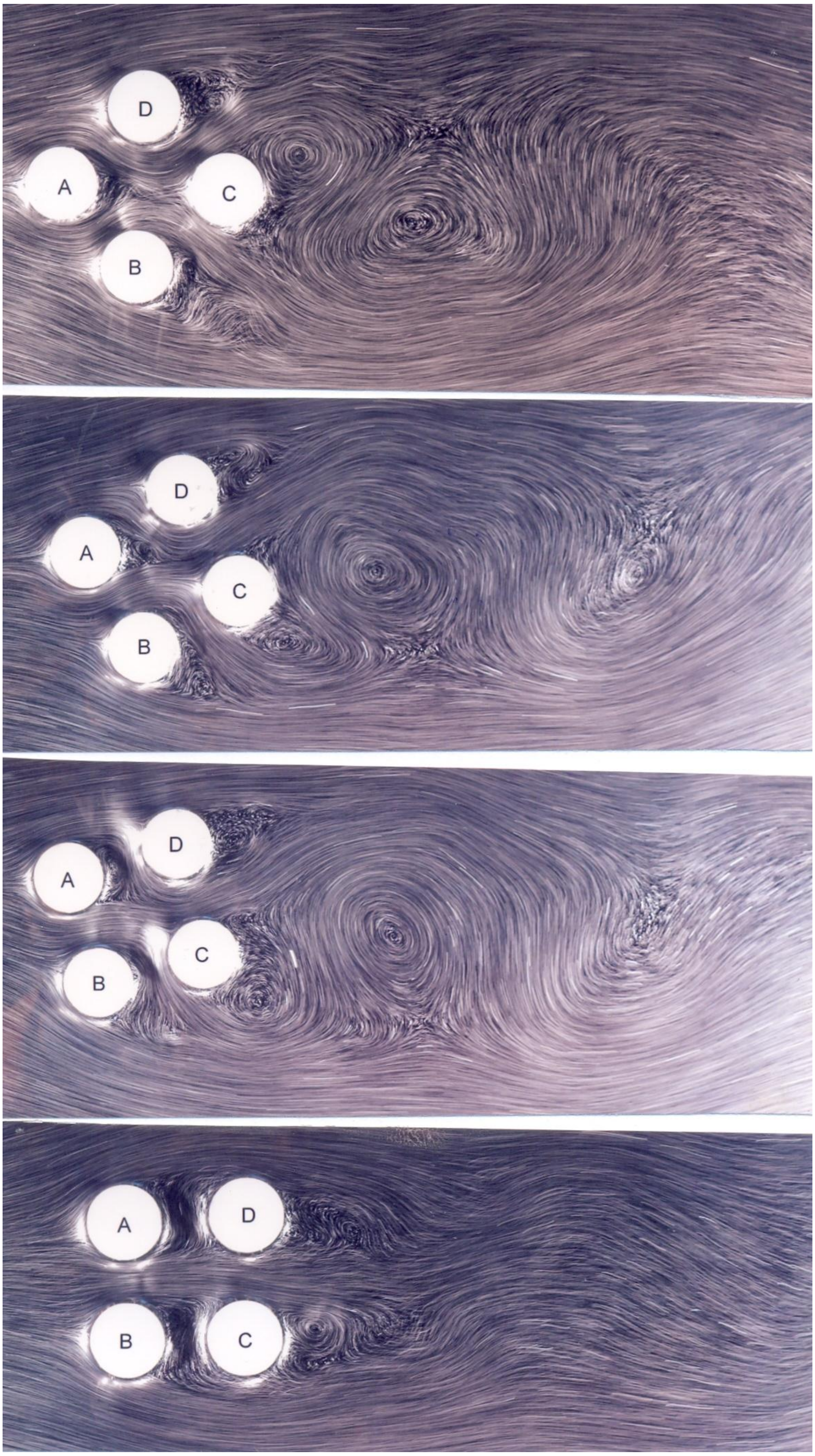

(a) $\alpha = 0^0$

(b) $\alpha = 15^0$

(c) $\alpha = 30^0$

(d) $\alpha = 45^0$

Fig.6 Flow pattern for various angle of attack α, g/d = 0.6

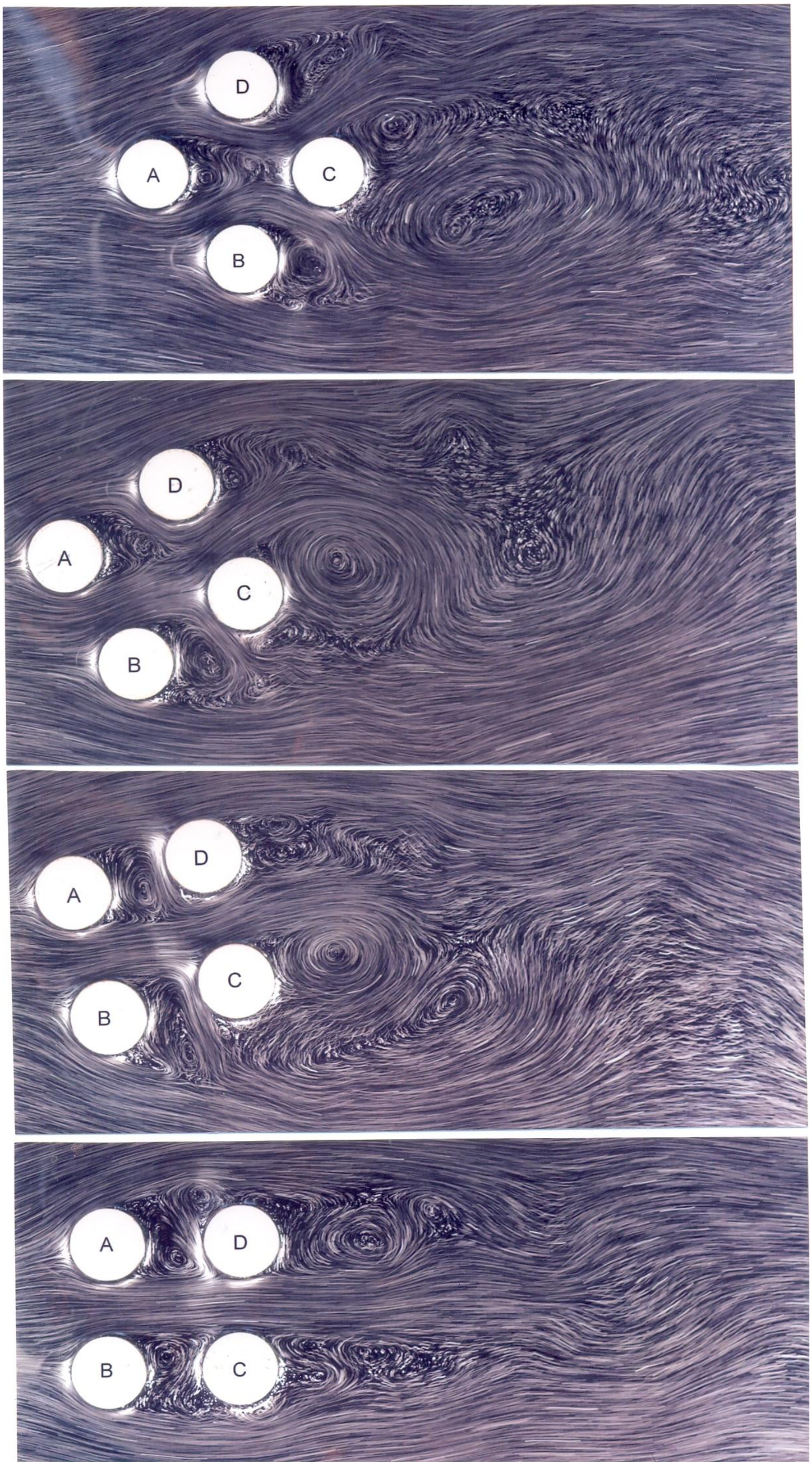

(a) $\alpha = 0^0$

(b) $\alpha = 15^0$

(c) $\alpha = 35^0$

(d) $\alpha = 45^0$

Fig.7 Flow pattern for various angle of attack α, g/d = 0.8

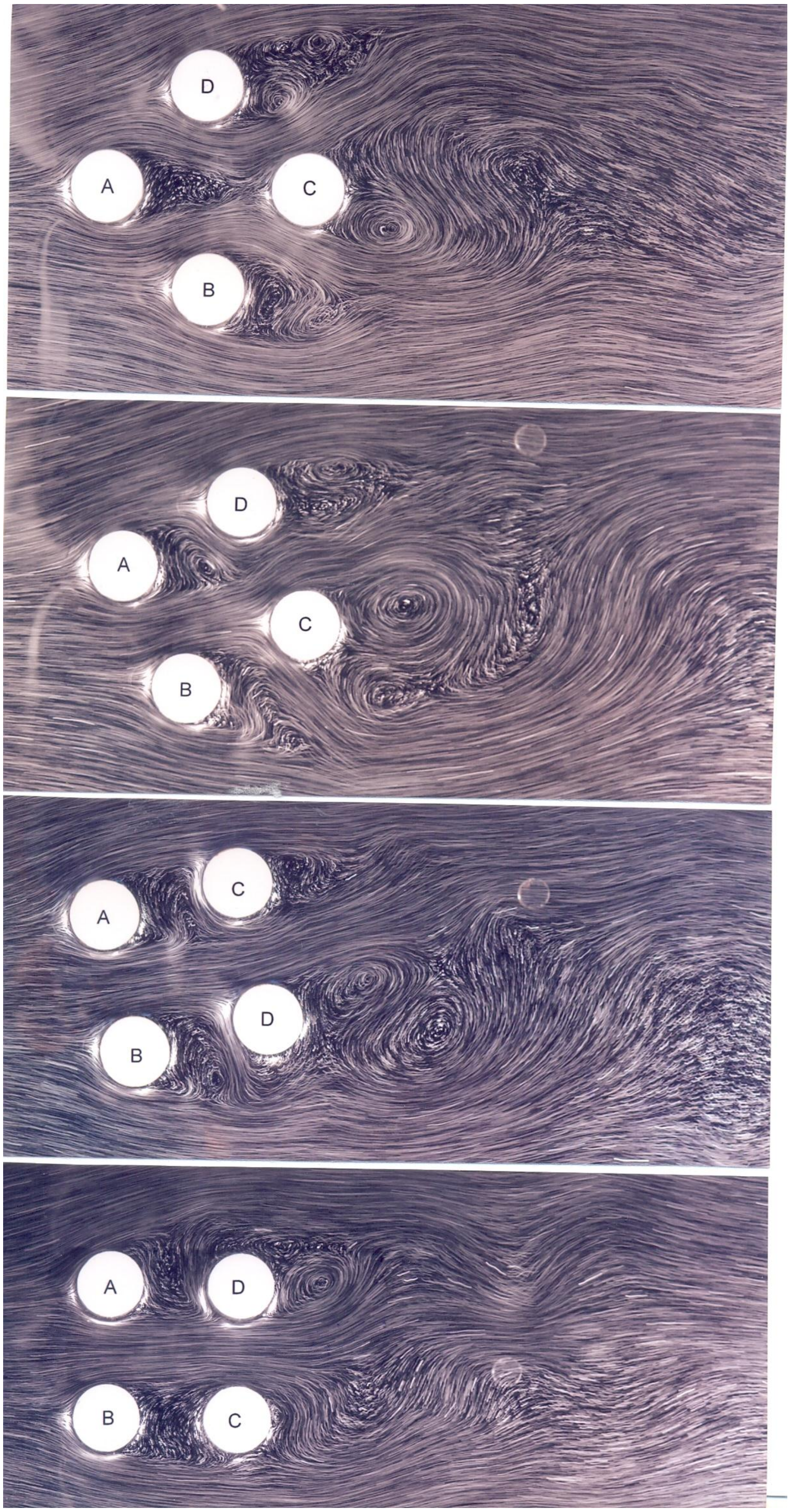

(a) $\alpha = 0^0$

(b) $\alpha = 15^0$

(c) $\alpha = 30^0$

(d) $\alpha = 45^0$

Fig.8 Flow pattern for various angle of attack α, g/d = 1